

# UC Berkeley

## UC Berkeley Previously Published Works

### Title

Modeling Iridium-Based Trilayer and Bilayer Transition-Edge Sensors

### Permalink

<https://escholarship.org/uc/item/3j226783>

### Journal

IEEE Transactions on Applied Superconductivity, 27(4)

### ISSN

1051-8223

### Authors

Wang, Gensheng  
Beeman, Jeffrey  
Chang, Clarence L  
et al.

### Publication Date

2017

### DOI

10.1109/tasc.2016.2646373

### Peer reviewed

# Modeling Iridium-Based Trilayer and Bilayer Transition-Edge Sensors

Gensheng Wang, Jeffrey Beeman, Clarence L. Chang, Junjia Ding, A. Drobizhev, B. K. Fujikawa, K. Han, S. Han, R. Hennings-Yeomans, Goran Karapetrov, Yury G. Kolomensky, Valentyn Novosad, T. O'Donnell, J. L. Ouellet, John Pearson, B. Sheff, V. Singh, S. Wagaarachchi, J. G. Wallig, and Volodymyr G. Yefremenko

**Abstract**—We report a model that can be used to calculate superconducting transition temperature of a transition-edge sensor (TES), which is either a normal metal–superconductor–normal metal trilayer or a normal metal–superconductor bilayer. The model allows the  $T_C$  estimation of a trilayer when the normal metals at the bottom and at the top are different. Furthermore, the model includes the spin flip time of the normal metals. We use the  $T_C$  calculations from this model for selected Ir-based trilayers and bilayers to help understand potential designs of low  $T_C$  TESs. A Au/Ir/Au trilayer can have a low  $T_C$  because the superconducting

order parameter is reduced with normal metals at both sides. On the other hand, an Ir/Pt bilayer can have a low  $T_C$  because the much larger electron density of states of Pt reduces the superconducting order parameter more effectively. Moreover, the spin flip scattering of paramagnetic Pt also contributes to the  $T_C$  reduction.

**Index Terms**—Superconductivity, proximity effect, transition-edge sensor, Usadel equations.

## I. INTRODUCTION

Manuscript received September 7, 2016; accepted December 22, 2016. Date of publication January 5, 2017; date of current version January 20, 2017. The work at the Argonne National Laboratory, including the use of facility at the Center for Nanoscale Materials, was supported in part by the Office of Science and in part by the Office of Basic Energy Sciences of the U.S. Department of Energy under Contract DE-AC02-06CH11357. (*Corresponding author: Gensheng Wang.*)

G. Wang and V. G. Yefremenko are with the High Energy Physics Division, Argonne National Laboratory, Lemont, IL 60439 USA (e-mail: gwang@anl.gov; yefremenko@anl.gov).

J. Beeman is with the Materials Science Division, Lawrence Berkeley National Laboratory, Berkeley, CA 94720 USA (e-mail: JWBeeman@lbl.gov).

C. L. Chang is with the High Energy Physics Division, Argonne National Laboratory, Lemont, IL 60439 USA, and also with the Kavli Institute for Cosmological Physics and Department of Astronomy and Astrophysics, University of Chicago, Chicago, IL 60637 USA (e-mail: clchang@kicp.uchicago.edu).

J. Ding, V. Novosad, and J. Pearson are with the Materials Science Division, Argonne National Laboratory, Lemont, IL 60439 USA (e-mail: dingj@anl.gov; novosad@anl.gov; pearson@anl.gov).

A. Drobizhev, R. Hennings-Yeomans, T. O'Donnell, and S. Wagaarachchi are with the Department of Physics, University of California, Berkeley, CA 94720 USA, and also with the Nuclear Science Division, Lawrence Berkeley National Laboratory, Berkeley, CA 94720 USA (e-mail: lyoshadrobizhev@berkeley.edu; hennings@berkeley.edu; tdonnell@berkeley.edu; sach@berkeley.edu).

B. K. Fujikawa is with the Nuclear Science Division, Lawrence Berkeley National Laboratory, Berkeley, CA 94720 USA (e-mail: bkfujikawa@lbl.gov).

K. Han is with the Department of Physics, Yale University, New Haven, CT 06520 USA (e-mail: ke.han@yale.edu).

S. Han, B. Sheff, and V. Singh are with the Department of Physics, University of California, Berkeley, CA 94720 USA (e-mail: sojinsmilev2@berkeley.edu; ben1sheff@berkeley.edu; singhv@berkeley.edu).

G. Karapetrov is with the Physics Department, Drexel University, Philadelphia, PA 19104 USA (e-mail: goran@drexel.edu).

Y. G. Kolomensky is with the Department of Physics, University of California, Berkeley, CA 94720 USA, and also with the Nuclear Science Division and Physics Division, Lawrence Berkeley National Laboratory, Berkeley, CA 94720 USA (e-mail: YGKolomensky@lbl.gov).

J. L. Ouellet is with the Department of Physics, University of California, Berkeley, CA 94720 USA, and also with the Massachusetts Institute of Technology, Cambridge, MA 02139 USA (e-mail: ouelletj@mit.edu).

J. G. Wallig is with the Engineering Division, Lawrence Berkeley National Laboratory, Berkeley, CA 94720 USA (e-mail: jgwallig@lbl.gov).

Color versions of one or more of the figures in this paper are available online at <http://ieeexplore.ieee.org>.

Digital Object Identifier 10.1109/TASC.2016.2646373

**I**N LOW-BACKGROUND experiments exploring fundamental physics, such as cryogenic Neutrino-less Double Beta Decay (NLDBD) searches [1], [2] and Dark Matter (DM) particle searches [3], [4], the TES can be an ideal thermometer. First, its large bandwidth can help capture a signal pulse shape to identify the particle's type and to provide event position information. Second, low impedance TES can be multiplexed to tens of thousands of channels, which may improve scaling of the experimental mass. On the other hand, reproducible fabrication of a large number of TES with required low  $T_C$  is not trivial. We have been making Ir-based bilayer and trilayer low  $T_C$  TESs using the proximity effect. Previously it was found that to make an Ir/Au bilayer TES with  $T_C < 30$  mK, the substrate needs to be heated up to 500 °C during the sputtering deposition of the Ir film [5]. Recently it was observed that low  $T_C$  TESs can be made with substrates at room temperature: a Au(200 nm)/Ir(100 nm)/Au(200 nm) trilayer can have a  $T_C$  close to 20 mK, and an Ir(100 nm)/Pt(80 nm) bilayer can have a similarly low  $T_C$  [5]. This work is motivated to understand the  $T_C$  of an Ir-based trilayer or bilayer.

The proximity effect, with which transition temperature of a superconductor can be reduced with a normal metal, is historically understood as a boundary effect [6], [7]. But the theory cannot match data without adding in an artificial factor in the  $T_C$  prediction equations [8]. A modern realization is that the proximity effect can be understood with the Usadel theory [9] by introducing an interface resistance and by applying proper boundary conditions [10], [11].

In this paper, we solve the Usadel equations, which are parameterized with a pairing angle in the microscopic superconductivity theory. A comprehensive description of the Usadel equations and their boundary conditions can be found in references [12]–[14]. In Section II, by solving the Usadel equations with the thin films approximation, we extend the  $T_C$  calculation

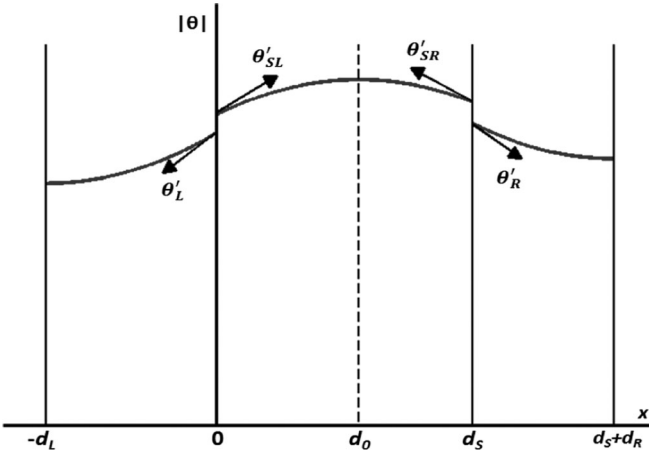


Fig. 1. The amplitude of the superconducting pairing parameter  $\theta$  vs position  $x$  for a NSN trilayer. The superconductor is from  $0$  to  $d_S$ . There are two metals. One is from  $-d_L$  to  $0$  on the left, another is from  $d_S$  to  $d_S + d_R$  on the right. The amplitude of  $\theta_S$  in the superconductor peaks at  $d_0$ , where  $\theta'_S = 0$ .

method of a bilayer in [14] to that of a NSN trilayer and include the effects due to spin flip scattering in the normal metals. We will estimate transition temperatures of an Ir/Au bilayer, an Ir/Pt bilayer, a Au/Ir/Au trilayer, and a Pt/Ir/Au trilayer in Section III. We conclude in Section IV.

## II. TRANSITION TEMPERATURE OF A TRILAYER OR A BILAYER

A trilayer consists of a normal metal with a thickness of  $d_L$  on the left, a superconductor with a thickness of  $d_S$  and a transition temperature of  $T_{CS}$  in the middle, and a normal metal with a thickness of  $d_R$  on the right. See Fig. 1. In the dirty limit (electron mean free path is less than coherence length), the properties of a superconductor in contact with a metal can be described with the Usadel equations [10]–[14]. In microscopic theory, the superconducting state is described by a function  $\theta(x, E)$  called the pairing angle, where  $x$  is a position coordinate and  $E$  is energy. The variable  $\theta$  is complex and ranges in magnitude from  $0$  to  $\pi/2$ .  $\theta = 0$  corresponds to the normal state. The Usadel equations used to solve for  $\theta(x, E)$  are

$$\frac{\hbar D_S}{2} \frac{\partial^2 \theta_S}{\partial x^2} + iE \sin \theta_S - \left[ \frac{\hbar}{\tau} + \frac{\hbar D_S}{2} \left( \frac{\partial \varphi}{\partial x} + \frac{2e}{\hbar} A_x \right)^2 \right] \times \cos \theta_S \sin \theta_S + \Delta(x) \cos \theta_S = 0, \quad (1)$$

and

$$\Delta(x) = N_S V_{\text{eff}} \int_0^{\hbar \omega_D} dE \tanh(E/2k_B T) \text{Im}[\sin \theta_S], \quad (2)$$

where  $D_S = \sigma_S/N_S e^2$  is the diffusivity of the superconductor,  $N_S$  is the density of states at the Fermi energy,  $\sigma_S$  is the normal state conductivity, and  $e$  is the electron charge.  $\varphi$  is the usual superconducting phase parameter.  $A_x$  is the vector potential.  $\tau$  is the electron spin-flip time.  $\Delta(x)$  is the superconducting order parameter.  $V_{\text{eff}}$  is the BCS-like interaction potential.  $\hbar$  is the reduced Plank constant.  $\omega_D$  is the Debye frequency.  $k_B$  is the Boltzmann constant. And  $T$  is the temperature.

In the equation (1), the spin-flip scattering, current ( $\partial \varphi / \partial x$  term) and magnetic field contribute to pair breaking [14]. With a small current and in absence of an external magnetic field, only the spin-flip time in paramagnetic metals [15]–[17] needs to be kept in a proximity effect analysis [18]–[20]. Near the  $T_C$  of a trilayer, the pairing angle satisfies  $|\theta| \ll 1$  in all three layers. It's assumed that each film is thinner than its coherence length. Therefore, the pairing angle  $\theta$  is approximately the same (almost constant) in the film. In the following calculations, we only include the dependence of  $\theta$  on  $x$  up to quadrature term ( $\partial \theta^2 / \partial x^2$  is constant) [14]. In the superconductor ( $0 < x < d_S$  in Fig. 1), it's assumed that the electron has no spin-flip scattering. The equation (1) can then be linearized as

$$\frac{\hbar D_S}{2} \frac{\partial^2 \theta_S}{\partial x^2} + iE \theta_S + \Delta(x) = 0. \quad (3)$$

For the normal metals ( $-d_L < x < 0$  and  $d_S < x < d_S + d_R$  in Fig. 1),  $V_{\text{eff}} = 0$ . By linearizing the equation (1), the paring angle parameter  $\theta_L$  or  $\theta_R$  satisfies

$$\frac{\hbar D_{L,R}}{2} \frac{\partial^2 \theta_{L,R}}{\partial x^2} + iE \theta_{L,R} - \frac{\hbar}{\tau_{L,R}} \theta_{L,R} = 0, \quad (4)$$

where  $D_L = \sigma_L/N_L e^2$  and  $D_R = \sigma_R/N_R e^2$  are the diffusivities of the normal metals on the left and on the right respectively,  $N_L$  and  $N_R$  are the density of states at the Fermi energies respectively, and  $\sigma_L$  and  $\sigma_R$  are the normal state conductivities respectively. Electron spin-flip times  $\tau_L$  and  $\tau_R$  are kept for potential paramagnetic property in normal metals [15]–[20].

The equations (3) and (4) are complemented with boundary conditions [10]–[14]. There are two kinds of boundaries. The first kind of boundary faces a vacuum or a dielectric. There is no current flowing out. Therefore,  $\partial \theta_L / \partial x = 0$  at  $x = -d_L$  and  $\partial \theta_R / \partial x = 0$  at  $x = d_S + d_R$  in Fig. 1.

The second kind of boundary connects two metals together. The current across the interface is conserved. Therefore, at the interface  $x = 0$ ,

$$\sigma_S \frac{\partial \theta_{SL}}{\partial x} = \sigma_L \frac{\partial \theta_L}{\partial x} = g_L (\theta_{SL} - \theta_L), \quad (5)$$

where  $g_L = G_L/A$ .  $A$  is the area of the interface.  $G_L = 2t_L N_{Ch} G_K$  is the interface conductance between the normal metal on the left and the superconductor, where  $t_L$  is a free parameter describing electron transmission coefficient across the interface,  $N_{Ch} = A/(\lambda_f/2)^2$  is the number of conductance channels, and  $\lambda_f$  is the Fermi wavelength in the metal or the superconductor that has fewer conductance channels, and  $G_K = e^2/h$  is the conductance quantum. Similarly, at the interface where  $x = d_S$ ,

$$\sigma_S \frac{\partial \theta_{SR}}{\partial x} = \sigma_R \frac{\partial \theta_R}{\partial x} = g_R (\theta_R - \theta_{SR}), \quad (6)$$

where  $g_R = G_R/A$ .  $G_R = 2t_R N_{Ch} G_K$  is the interface conductance between the normal metal on the right and the superconductor, where  $t_R$  is a free parameter describing electron transmission coefficient across the interface.

By applying the boundary condition  $\partial \theta_L / \partial x = 0$  at  $x = -d_L$ , it's found that  $\partial \theta_L / \partial x = d_L (\partial \theta_L^2 / \partial x^2)$  at  $x = 0$ . By applying the boundary condition  $\partial \theta_R / \partial x = 0$

at  $x = d_S + d_R$ , it's found that  $\partial\theta_R/\partial x = -d_R(\partial\theta_R^2/\partial x^2)$  at  $x = d_S$ . By utilizing the equation (4), the pairing angle  $\theta_L$  at  $x = 0$  or the pairing angle  $\theta_R$  at  $x = d_S$  satisfies

$$\frac{\partial\theta_{L,R}}{\partial x} = \mp \left( iE - \frac{\hbar}{\tau_{L,R}} \right) \theta_{L,R} \frac{2d_{L,R}}{\hbar D_{L,R}}, \quad (7)$$

where the “–” sign in the equation is for  $\theta_L$  at  $x = 0$  and the “+” sign is for  $\theta_R$  at  $x = d_S$ .

In the superconductor, the calculation is simplified with the approximation that the small  $\theta_S$  near the  $T_C$  only depends on  $x$  up to the quadrature term. The amplitude of  $\theta_S$  peaks at  $d_0$ , therefore,  $\partial\theta_S/\partial x = 0$  at  $x = d_0$ . It's straightforward to find that  $\partial\theta_{SL}/\partial x = -d_0(\partial\theta_S^2/\partial x^2)$  at  $x = 0$  and  $\partial\theta_{SR}/\partial x = (d_S - d_0)(\partial\theta_S^2/\partial x^2)$  at  $x = d_S$ . By utilizing the equation (3), the pairing angle  $\theta_{SL}$  at  $x = 0$  or the pairing angle  $\theta_{SR}$  at  $x = d_S$  satisfies

$$\frac{\partial\theta_{SL,SR}}{\partial x} = \pm (iE\theta_S + \Delta) \frac{2d_X}{\hbar D_S}, \quad (8)$$

where the “+” sign with  $d_X = d_0$  in the equation is for  $\theta_{SL}$  at  $x = 0$ , the “–” sign with  $d_X = d_S - d_0$  is for  $\theta_{SR}$  at  $x = d_S$ . Note that the same  $\theta_S$  is used in the equation (8) for both  $\theta_{SL}$  and  $\theta_{SR}$ , which means the  $\theta_S$  is approximately constant in the thin superconducting film.  $d_0$  and  $\theta_S$  can be found by solving equations (5)–(8). Both  $d_0$  and  $\theta_S$  depend on energy  $E$ .

An electron coherence length can be defined at a low frequency approximation  $E = i\omega$ , where  $\omega = \pi k_B T$  is Matsubara frequency at the lowest order [6], [7]. In the equation (7), the coherence length of the normal metal on the left or on the right in Fig. 1 is  $\xi_{L,R} = \sqrt{\hbar D_{L,R}/2\pi k_B T(1 + \hbar/\pi k_B T\tau_{L,R})}$ . In the equation (8), the coherence length of the superconductor in the middle without spin-flip scattering is  $\xi_S = \sqrt{\hbar D_S/2\pi k_B T}$ . The coherence length aids in understanding the material characteristics and calculation results in next section.

To continue the modeling without a low frequency approximation,  $\theta_S$  can be written as

$$\theta_S = \frac{i\Delta}{E} (1 - (f_A + if_B)), \quad (9)$$

with

$$f_A + if_B = \frac{1}{1 - iEd_S f_1 f_2 / (f_1 + f_2)}, \quad (10)$$

where  $f_A$  and  $f_B$  are real numbers. The functions  $f_1$  and  $f_2$  are

$$f_{1,2} = a_{L,R} N_S - \frac{1}{iE - \hbar/\tau_{L,R}} \frac{N_S}{N_{L,R}} \frac{1}{d_{L,R}}, \quad (11)$$

where  $a_L = 4\pi G_K/g_L$  and  $a_R = 4\pi G_K/g_R$ .

Taking the imaginary part of  $\theta_S$  in the equation (9) and inserting into the order parameter equation (2), it's found that

$$\frac{1}{N_S V_{\text{eff}}} = \int_0^{\hbar\omega_D} \frac{dE}{E} (1 - f_A) \tanh \left( \frac{E}{2k_B T_C} \right). \quad (12)$$

The first term in the equation (12) is the electron-phonon interaction in the superconductor film, which defines  $T_{CS}$ . The second term is a modification of the electron-phonon interaction due to the normal metal and superconductor contact. So, the  $T_C$

TABLE I  
PHYSICAL PARAMETERS FOR  $T_C$  CALCULATIONS

Parameter	Ir	Au	Pt
Electron phonon coupling constant $\lambda$ <sup>a,b</sup>	0.34	0.17	0.60
Electronic specific heat $\gamma$ in $\text{JK}^{-2} \text{m}^{-3}$ <sup>a,b</sup>	$3.70 \times 10^2$	$7.15 \times 10^1$	$7.29 \times 10^2$
Fermi wavelength $\lambda_f$ in nm <sup>c</sup>	0.536	0.518	0.609
Resistivity at 300 K $\rho_{300}$ in $10^{-8} \Omega \text{ m}$ <sup>d,e</sup>	5.2	2.2	10.9
Debye temperature $\theta_D$ in Kelvin <sup>f</sup>	420	165	240
Electron coherence length $\xi$ in nm <sup>g</sup>	379	1355	194

<sup>a</sup>Ref. [21]; <sup>b</sup>Ref. [22]; <sup>c</sup>Ref. [23]; <sup>d</sup>Ref. [24]; <sup>e</sup>Ref. [25]; <sup>f</sup>Ref. [26].

<sup>g</sup> $\xi = \sqrt{\hbar D/2\pi k_B T} = \sqrt{\hbar\pi k_B 6e^2 \gamma\rho T}$  [27], where  $T = 30 \text{ mK}$ .

of the NSN trilayer can be found with

$$\ln \left( \frac{T_C}{T_{CS}} \right) = - \int_0^{\hbar\omega_D} \frac{dE}{E} (f_A) \tanh \left( \frac{E}{2k_B T_C} \right), \quad (13)$$

where  $f_A$  is calculated using the equations (10)–(11). The  $T_C$  can be calculated with an iterative method.

For a NS bilayer consisting of a normal metal where  $-d_L < x < 0$  and a superconductor where  $0 < x < d_0$  in Fig. 1, we solve the equation (5), the equation (7) with the “–” sign, and the equation (8) the “+” sign for  $\theta_S$  in the superconductor. We can write  $\theta_S$  in the form of equation (9) with

$$f_A = \frac{f_1}{1 + f_2^2}, \quad (14)$$

where

$$f_1 = \frac{1 + \frac{\hbar^2}{(E\tau_L)^2}}{1 + \frac{\hbar^2}{(E\tau_L)^2} + \frac{d_0 N_S}{d_L N_L}}, \quad (15)$$

and

$$f_2 = \frac{\left(1 + \frac{\hbar^2}{(E\tau_L)^2}\right) d_0 N_S E a_L + \frac{\hbar}{E\tau_L} \frac{d_0 N_S}{d_L N_L}}{1 + \frac{\hbar^2}{(E\tau_L)^2} + \frac{d_0 N_S}{d_L N_L}}. \quad (16)$$

So, the  $T_C$  of a NS bilayer can be estimated using the equation (13), where  $f_A$  is calculated with the equations (14)–(16).

The calculations above are for the normal metals with a large electron spin flip rate  $1/\tau_L$ . At a small spin flip rate,  $\hbar/E\tau_L \ll 1$ , it can be verified that the equation (13) can be simplified to the equation (7) in [14], which is for the  $T_C$  calculation of a non-magnetic metal superconductor bilayer.

### III. $T_C$ CALCULATION OF NSN TRILAYERS AND NS BILAYERS

We calculate the transition temperatures of Ir/Au and Ir/Pt bilayers using the equations (13) and (14)–(16), and that of Au/Ir/Au and Pt/Ir/Au trilayers using the equations (13) and (10)–(11). The input physical parameters from literature [21]–[26] are listed in Table I. The electron coherence length is also estimated in the table. We use electron specific heat density of states,  $N_{N,S} = 3\gamma_{N,S}/\pi^2 k_B^2 (1 + \lambda_{N,S})$  [26] for the normal metals N and the superconductor S. In addition, we assume the residual resistance ratio  $RRR = 3$  for all films. The electron conductivity  $\sigma = 1/\rho$  and  $\rho = \rho_{300}/RRR$ .

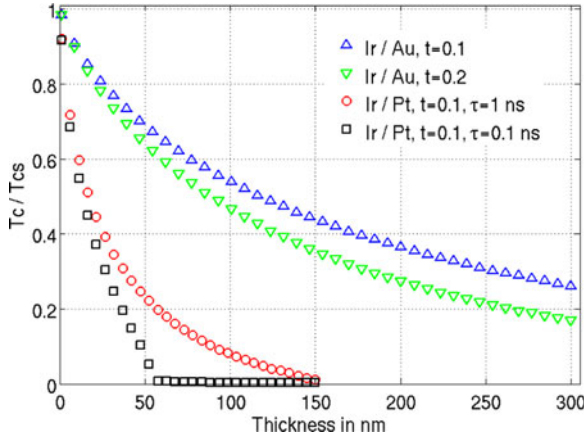


Fig. 2. The  $T_C$  of Ir/Au and Ir/Pt bilayers normalized to  $T_{CS}$ . Ir film is 100 nm thick for all the four curves.  $t$  in the legend is for the electron transmission coefficient across the interface.  $\tau$  is for electron spin flip time in Pt.

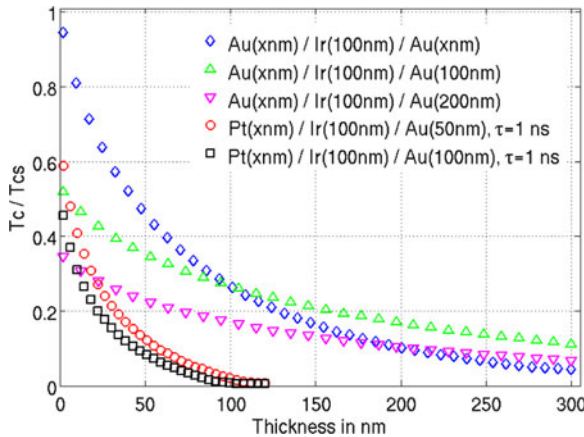


Fig. 3. The  $T_C$  of Au/Ir/Au and Pt/Ir/Au trilayers normalized to  $T_{CS}$ . The electron transmission coefficient across the interface is  $t = 0.1$  for all the five curves.  $\tau$  is for electron spin flip time in Pt.

Fig. 2 shows the transition temperatures normalized to the bare superconducting film's  $T_{CS}$  for Ir/Au and Ir/Pt bilayers. The blue triangles and the green inverse triangles demonstrate that the  $T_C$  of a NS bilayer is lower when the electron transmission coefficient across the interface is larger. The result is consistent with other studies [13], [28]–[30]. It is also observed that a Pt film suppresses the  $T_C$  of an Ir film more strongly than a Au film does. The observation is related to both the large specific heat coefficient and the strong paramagnetic property of Pt [31], [32]. First, the one order of magnitude larger electron density of states (which is calculated with  $\lambda$  and  $\gamma$  data in Table I) in Pt than in Au enhances the  $T_C$  suppression. Secondly, the paramagnetic effect in Pt, whose strength is characterized with a spin-flip time, suppresses cooper pairs. Note that a spin-flip time  $\tau = 0.08$  ns corresponds to  $\hbar/\pi k_B T \tau \approx 1$  at  $T = 30$  mK. A spin-flip time  $\tau$  larger than 1 ns, which corresponds to  $\hbar/\pi k_B T \tau \ll 1$ , has a negligible impact to the  $T_C$  of an Ir/Pt bilayer.

Fig. 3 shows the transition temperatures normalized to the bare superconducting film's  $T_{CS}$  for Au/Ir/Au and Pt/Ir/Au

trilayers. By comparing the blue diamonds in Fig. 3 and the blue triangles in Fig. 2, it's realized that the Ir film's  $T_C$  is suppressed more effectively when Au films are used at both sides of an Ir film. This strategy in making a low  $T_C$  TES is important when an Ir film's  $T_C$  is high. For example, thin Ir films sputtered at room temperature can have a fairly high  $T_C$  [33], [34], but there are advantages in making a TES without substrate heating. By comparing the  $T_C$  data of Ir/Au and Ir/Pt bilayers in Fig. 2 as well as the resistivity and specific heat coefficient data in Table I, it may make sense to use a Pt/Ir/Au trilayer. A Pt film, which has a high resistivity and a large specific heat ( $c = \gamma T$  for a metal. See Table I for  $\gamma$  data), can be used to control the  $T_C$  of a TES at the bottom. A Au film, which has low resistivity and a small specific heat can be used as a passivation layer on the top. As such, while the low  $T_C$  of a TES is well defined, there is an additional adjustability in its resistance or heat capacity. The transition temperatures as a function of Pt film thickness for two Pt/Ir/Au configurations are shown in Fig. 3 as the red circles and black squares.

#### IV. CONCLUSION

By solving the microscopic Usadel equations with proper boundary conditions, the  $T_C$  calculation methods of an NSN trilayer and a NS bilayer are developed. Material properties such as electron density of states, electron transmission efficiency across the interface of metals and electron spin-flip time of normal metals are included in the methods. The transition temperatures of Ir-based bilayers and trilayers are calculated with physical parameters available from the literature. There are several options to make an Ir-based low  $T_C$  TES without substrate heating. They can be an Ir/Pt bilayer, a Pt/Ir/Au trilayer and a Au/Ir/Au trilayer respectively.

#### REFERENCES

- [1] K. Alfonso *et al.*, “Search for neutrinoless double-beta decay of  $^{130}\text{Te}$  with CUORE-0,” *Phys. Rev. Lett.*, vol. 115, 2015, Art. no. 102502.
- [2] G. Wang *et al.*, “R&D towards CUPID (CUORE Upgrade with Particle Identification),” 2015. [Online]. Available: <http://arxiv.org/pdf/1504.03612v1.pdf>
- [3] Z. Ahmed *et al.*, “Search for weakly interacting massive particles with the first five-tower data from the cryogenic dark matter search at the Soudan underground laboratory,” *Phys. Rev. Lett.*, vol. 102, 2009, Art. no. 011301.
- [4] G. Angloher *et al.*, “Results from 730 kg days of the CRESST-II dark matter search,” *Eur. Phys. J. C*, vol. 72, 2012, Art. no. 1971.
- [5] R. Hennings-Yeomans *et al.*, “Development of low-Tc transition edge sensors for neutrino-less double beta decay,” in *Proc. Appl. Supercond. Conf.*, Denver, CO, USA, Sep. 4–9, 2016, Paper 1EOr3C-01.
- [6] N. R. Werthamer, “Theory of the superconducting transition temperature and energy gap function of superposed metal films,” *Phys. Rev.*, vol. 132, no. 6, pp. 2440–2445, 1963.
- [7] P. G. de Gennes, “Boundary effects in superconductors,” *Rev. Mod. Phys.*, vol. 36, pp. 225–237, 1964.
- [8] U. Nagel *et al.*, “Proximity effect in iridium-gold bilayers,” *J. Appl. Phys.*, vol. 110, 1994, Art. no. 063919.
- [9] K. D. Usadel, “Generalized diffusion equation for superconducting alloys,” *Phys. Rev. Lett.*, vol. 25, pp. 507–509, 1970.
- [10] M. Yu. Kupriyanov and V. F. Lukichev, “Influence of boundary transparency on the critical current of ‘dirty’ SS'S structures,” *Sov. Phys. JETP*, vol. 67, pp. 1163–1168, 1988.
- [11] A. A. Golubov, M. Y. Kupriyanov, and E. Il'ichev, “The current-phase relation in Josephson junctions,” *Rev. Mod. Phys.*, vol. 76, pp. 411–469, 2004.

- [12] S. Gueron, H. Pothier, N. O. Birge, D. Esteve, and M. H. Devoret, "Superconducting proximity effect probed on a mesoscopic length scale," *Phys. Rev. Lett.*, vol. 77, no. 14, pp. 3025–3028, 1996.
- [13] Y. V. Fominov and M. V. Feigel'man, "Superconductive properties of thin dirty superconductor-normal metal bilayers," *Phys. Rev. B*, vol. 63, 2001, Art. no. 094518.
- [14] J. M. Martinis, G. C. Hilton, K. D. Irwin, and D. A. Wollman, "Calculation of  $T_C$  in a normal-superconductor bilayer using the microscopic-based Usadel theory," *Nuclear Instrum. Methods Phys. Res., Section A*, vol. 444, no. 1/2, pp. 23–27, 2000.
- [15] D. Katayama, A. Sumiyama, and Y. Oda, "Proximity-induced superconductivity in platinum metals," *Phys. Rev. B*, vol. 68, 2003, Art. no. 132502.
- [16] T. Herrmannsdörfer, S. Rehmann, W. Wendler, and F. Pobell, "Magnetic properties of highly diluted PdFex and PtFex alloys. Part I. Magnetization at Kelvin temperatures," *J. Low Temp. Phys.*, vol. 104, no. 1/2, pp. 49–65, 1996.
- [17] T. Herrmannsdörfer, S. Rehmann, and F. Pobell, "Magnetic properties of highly diluted PdFex and PtFex alloys. Part II. Susceptibility at Micro- and Milli-Kelvin temperature," *J. Low Temp. Phys.*, vol. 104, no. 1/2, pp. 67–94, 1996.
- [18] T. Kontos, M. Aprili, J. Lesueur, X. Grison, and L. Dumoulin, "Superconducting proximity effect at the paramagnetic-ferromagnetic transition," *Phys. Rev. Lett.*, vol. 93, 2004, Art. no. 137001.
- [19] O. Entin-Wohlman, "Proximity effects between superconducting and magnetic films," *Phys. Rev. B*, vol. 12, no. 11, pp. 4860–4866, 1975.
- [20] J. J. Hauser, H. C. Theuerer, and N. R. Werthamer, "Proximity effects between superconducting and magnetic films," *Phys. Rev.*, vol. 142, no. 1, pp. 118–126, 1966.
- [21] W. John, V. V. Nemosilkalenko, V. N. Antonov, and VL. N. Antonov, "Electron phonon interaction in transition metals, results of relativistic APW band structure calculations," *Phys. Status Solidi (b)*, vol. 121, pp. 233–239, 1984.
- [22] Z. Lin, L. V. Zhigilei, and V. Celli, "Electron-phonon coupling and electron heat capacity of metals under conditions of strong electron-phonon nonequilibrium," *Phys. Rev. B*, vol. 77, 2008, Art. no. 075133.
- [23] C. Reale, "Conductivity data for the transition metals derived from considerations on the charge transport in thin films," *J. Phys. F*, vol. 4, pp. 2218–2222, 1974.
- [24] D. Gall, "Electron mean free path in elemental metals," *J. Appl. Phys.*, vol. 119, 2016, Art. no. 085101.
- [25] J. W. Arblaster, "Selected electrical resistivity values for platinum group of metals part I: Palladium and platinum," *Johnson Matthey Technol. Rev.*, vol. 59, pp. 174–181, 2015.
- [26] C. Kittel, *Introduction to Solid State Physics*, 7th ed. Hoboken, NJ, USA: Wiley, 1996.
- [27] J. J. Hauser, N. R. Werthamer, and H. C. Theuerer, "Superconductivity in Cu + Pb by means of superimposed films with lead," *Phys. Rev. A*, vol. 136, no. 3A, pp. A637–A641, 1964.
- [28] A. A. Golubov, "Proximity effect in dirty N/S multilayers," *Proc. SPIE*, vol. 2157, pp. 353–362, 1994.
- [29] C. Cirillo, S. L. Prischepa, M. Salvato, and C. Attanasio, "Interface transparency of Nb/Pd layered systems," *Eur. Phys. J. B*, vol. 38, pp. 59–64, 2004.
- [30] R. Boucher, T. May, T. Wagner, V. Zakosarenko, S. Anders, and H. G. Mayer, "Structural and electrical properties of AuPd/Mo bi-layer films for transition edge sensors," *Supercond. Sci. Technol.*, vol. 19, pp. 138–142, 2006.
- [31] K. Andres and M. A. Jensen, "Superconductivity, susceptibility, and specific heat in the noble transition elements and alloys. I. Experimental results," *Phys. Rev.*, vol. 165, no. 2, pp. 533, 1968.
- [32] M. A. Jensen and K. Andres, "Superconductivity, susceptibility and specific heat in noble transition elements and alloys. 2. Comparison with theory," *Phys. Rev.*, vol. 165, no. 2, pp. 545–555, 1968.
- [33] D. Fukuda, H. Takahashi, M. Ohno, and M. Nakazawa, "Ir TES for X-ray microcalorimeters," *Nucl. Instrum. Methods A*, vol. 444, pp. 241–244, 2000.
- [34] M. Galeazzi, D. Bogorin, R. Molina, M. Ribiro Gomes, and T. Saab, "Detector development for the MARE neutrino experiment," *AIP Conf. Proc.*, vol. 1185, pp. 558–561, 2009.